Fully physical, time-dependent thermal modelling of complex 3-dimensional systems for device and circuit level electro-thermal CAD

W. Batty[×+], C. E. Christoffersen[*], S. David[×], A. J. Panks[×],
R. G. Johnson[×], C. M. Snowden[×] and M. B. Steer[*],

[×]Institute of Microwaves and Photonics,
School of Electronic and Electrical Engineering,
University of Leeds, Leeds LS2 9JT, UK.

[*]Department of Electrical and Computer Engineering,
North Carolina State University (NCSU),
Raleigh, NC 27695-7914, USA.

[+]Contact author:
tel. +44 113 2332089, fax +44 113 2332032, e-mail w.batty@elec-eng.leeds.ac.uk

Abstract— **An original spectral domain decomposition approach, to solution of the time-dependent heat diffusion equation in complex volumes, is introduced. Its application to device and circuit level electro-thermal simulation on CAD timescales is outlined. The first full treatment in coupled electro-thermal CAD, of thermal non linearity due to temperature dependent diffusivity, is described. Original thermal solutions are presented in the form of analytically exact thermal impedance matrix expressions for thermal subsystems. These include time domain expressions for MMICs, found to be rapidly convergent for all times, and original double Fourier series solutions for the case of arbitrarily distributed volume heat sources and sinks, constructed without the use of Green's function techniques. The time-independent thermal resistance matrix approach is illustrated by a fully physical, coupled electro-thermal device study of the interaction of substrate thickness and surface convection in power HEMTs. The thermal time-dependent implementation is illustrated by circuit level transient simulation of a 3×3 MMIC amplifier array.**

I. Introduction

Solutions of the heat diffusion equation for complex 3-dimensional systems are commonly based on finite volume, finite element, finite difference or boundary element methods. All of these approaches require construction of a volume or surface mesh. They are computationally intensive and therefore generally unsuitable for direct implementation in the necessarily iterative solution of intrinsically non linear coupled electro-thermal problems. In this paper, a new approach is presented to the solution of the time-dependent heat diffusion equation in complex 3-dimensional volumes. Generically, this approach is a spectral domain decomposition technique [1]. Simple composite systems have been treated previously by the Unsteady Surface Element (USE) method of Beck *et al.*, [2], and this approach has the advantage that it only discretises interfaces between subsystems. Like the USE method, the approach presented here discretises only interfaces (and heating elements). It constructs solutions for thermal subvolumes which are fully analytical, with development of double Fourier series solutions for thermal subvolumes by explicit construction of series expansion coefficients. Thus it differs from semi-analytical Fourier approaches for simple rectangular multilayers [3], based on collocation or function sampling, which require numerical manipulation such as DFT-FFT to generate expansion coefficients. As solutions for subvolumes are fully analytical, no volume or surface mesh is required. Global solutions for complex volumes are constructed by matching of temperature and flux at subvolume interfaces. Such solutions are applicable for describing complex structures, from metallised, multigate power FETs, through MMICs and MCMs, upto circuit board level. A particular intended application is the treatment of MMIC arrays for spatial power combining at millimeter wavelengths.

Importantly, this modular thermal solution is constructed to be compatible with coupled electro-thermal device and circuit simulation on CAD timescales. This is achieved by formulating the analytically exact subsystem solutions in terms of thermal impedance matrices. These thermal impedance matrices describe explicitly, only the temperature variation with time, in the vicinity of the power dissipating and interface regions required for coupling of the electrical and thermal problems. No redundant temperature information is generated on the surface or in the body of the subsystem volumes. As these minimal thermal solutions are generated analytically, the thermal impedance matrices are all precomputed, prior to the coupled electro-thermal simulation, purely from structural information. Thermal updates in the coupled electro-thermal problem are therefore rapid. However, each thermal impedance matrix corresponds to full analytical solution of the heat diffusion equation. Thus, once power dissipation of active elements has been obtained self-consistently, by coupled electro-thermal simulation, description of temperature variation at any instant, at any point within the body, or on the surface, of the complex 3-dimensional volume, can be obtained essentially exactly, for model validation by comparison against thermal measurements.

Fully coupled device level simulation can be be implemented by combination of this thermal impedance matrix model with any thermally self-consistent device model. If the device model includes self-heating effects, then the global thermal impedance matrix will provide an accurate, CAD timescale, description of mutual thermal interaction between power dissipating elements, however complex the thermal system. The matrix form of the analytical thermal solution for subsystems, means that global thermal impedance matrices can be expressed explicitly in terms of simple manipulations on subsystem matrices. Coupled electro-thermal solution is achieved by iterative solution of the electrical and thermal problems, with thermal updates provided by small matrix multiplications, and thermal non linearity transferred to the already non linear active device model. Fully physical, coupled electro-thermal simulations for the thermal time-independent and time-dependent cases, have been described by the authors previously [4]–[7]. These were based on coupling of the thermal model presented here, to the quasi-2-dimensional Leeds Physical Model of MESFETs and HEMTs [8]–[11].

Circuit implementation of this thermal solution, exploits the ability of network based microwave circuit simulators to describe multiport non linear elements in the time domain, and to treat distributed EM systems in terms of multiport network parameters [12]. The thermal solution makes use of the close analogy between distributed EM and

thermal systems. The magnetic vector potential equation in frequency space, is just the Helmholtz equation, as is the time-dependent heat diffusion equation in Laplace transform s-space (complex frequency space), after appropriate transformation of thermal non linearity. Double Fourier series thermal solutions resemble analytical EM Green's function solutions (and the same series acceleration techniques can be used in each case). Most importantly, complex EM systems are treated by segmentation [13] and cascading of subsystem solutions by use of network parameter matrices. The transformed (initially non linear) thermal problem is therefore immediately compatible with network based microwave circuit simulation engines, by interpretation of thermal impedance matrices, for distributed thermal subsystems, in terms of generalised multiport network parameters. Analytical, s-space solution for thermal subsystems, means that no numerical identification of thermal networks, such as that provided by the NID method [14], is required. It also means that each thermal subsystem can be described in either the time domain or in the frequency domain. In the time domain, the thermal subsystem is treated as a non linear multi-port element, which readily allows non linear matching of transformed temperatures at thermal subsystem interfaces [4], [5]. In the frequency domain, the thermal subsystem is represented by a matrix of complex phasors inserted into the modified nodal admittance matrix (MNAM) for the microwave system, and thermal non linearity is again transferred to the already non linear active device model. This gives coupled electro-thermal harmonic balance and transient solutions on CAD timescales. Coupled electro-thermal circuit level CAD generally requires thermal model reduction, *e.g.*, [15]–[17]. Rapidly convergent, fully analytical and minimal thermal impedance matrix expressions, in both the time and frequency domains, mean that no reduced, lumped element, RC network description, is required in the multiport network parameter approach. Analytical expressions for the multiport network parameters of all thermal subvolumes means that no distinct thermal simulator, separate from the coupled electro-thermal simulation engine, is required to characterise the complex thermal system. Such simulations have been described by the authors in [18] which outlines the coupling of the thermal model to microwave circuit simulator Transim (NCSU) [19].

A key aspect of the thermal solution presented here, is application of a generalised 'radiation' boundary condition, on the top and bottom surfaces of all thermal subvolumes, in the analytical subsystem solutions. This boundary condition allows analytical subsystem solutions with interface discretisation, and construction of global thermal solutions by vertical matching of temperatures and fluxes at subsystem interfaces. The boundary condition also allows integral treatment of surface radiation and convection. One aim of this paper is to present explicit analytical solutions for thermal subsystem impedance matrices, allowing global solution for complex systems. Generation of such solutions requires treatment of thermal non linearity inherent in temperature dependence of material parameters. An original treatment of this non linearity, for device and circuit level electro-thermal CAD, is presented first. This is followed by derivation of thermal impedance matrix solutions for a homogeneous MMIC, and an N-level rectangular multilayer. It is shown how the time-dependent form of the thermal impedance matrix can be expressed in a rapidly convergent form for all time, t. This is followed by presentation of an original double Fourier series solution to the time-dependent heat diffusion equation with arbitrarily distributed volume heat sources and sinks. This goes beyond previous solutions in the literature, which treat heat dissipating sources as planar, either at the surface or interfaces of rectangular multilayers [3]–[5]. Use of the thermal resistance matrix approach for the thermal time-independent case is then indicated by an illustrative, fully physical, electro-thermal device study of the relation between substrate thinning and the magnitude of surface convection in power HEMTs. Finally, implementation of the time-dependent thermal impedance matrix approach, in circuit level CAD, is illustrated by simulation of a 3×3 MMIC amplifier array.

II. Thermal non linearity

The time dependent heat diffusion equation is given by,

$$\nabla . [\kappa(T) \nabla T] + g = \rho C \frac{\partial T}{\partial t}, \tag{1}$$

where T is temperature, t is time, $\kappa(T)$ is temperature dependent thermal conductivity, $g(x, y, z, t)$ is rate of heat generation, ρ is density and C is specific heat. This equation is non linear through the temperature dependence of $\kappa(T)$ (and possibly of ρ and C). To linearise the equation, the Kirchhoff transformation is performed [20]. The equation for transformed temperature θ then becomes,

$$\nabla^2 \theta - \frac{1}{k(\theta)} \frac{\partial \theta}{\partial t} = -\frac{g}{\kappa_S}, \tag{2}$$

where $\kappa_S = \kappa(T_S)$ and diffusivity $k = \kappa / \rho C$. k is now a function of θ so the equation is still non linear. At this stage it is conventional, in electro-thermal simulations employing the Kirchhoff transformation, to assume that $k(\theta)$ is approximately constant, thus fully linearising the time-dependent heat diffusion equation. However, for typical semiconductor systems this assumption requires further examination. For GaAs, in temperature ranges of interest, thermal conductivity varies as [21],

$$\kappa(T) = \kappa_S \left(\frac{T}{T_S} \right)^{-1.22}. \tag{3}$$

Fig. 1 shows plots of $\kappa(T)$ against T (solid line) and $k(\theta)$ against θ (dashed line), both normalised to their values at $T = T_S$, assumed equal to 300 K. ρC has been assumed independent of θ, which is a good approximation for semiconductors. It is apparent that the Kirchhoff transformation does not remove the temperature sensitivity of the material parameters for the time-dependent case.

Defining a new time variable, τ, by [22]

$$k_S \tau = \int_0^t k(\theta) dt, \tag{4}$$

the time-dependent heat diffusion equation becomes finally,

$$\nabla^2 \theta - \frac{1}{k_S} \frac{\partial \theta}{\partial \tau} = -\frac{g}{\kappa_S}. \tag{5}$$

The fully linearised equation, Eq. (5), can now be solved exactly. To illustrate the significance of the time variable transformation, Eq. (4), for electro-thermal response, an analytical thermal impedance matrix is constructed to describe the response to step power input of 0.4 W, over a central square $0.1L \times 0.1L$, at the surface of a cubic GaAs

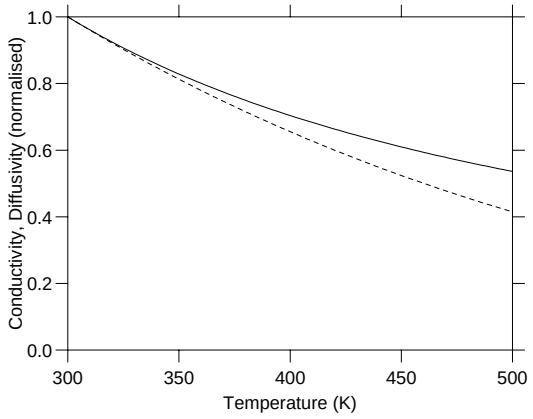

Fig. 1. Calculated temperature dependence of thermal conductivity, $\kappa(T)$, (solid line), and diffusivity, $k(\theta)$, (dashed line), in terms of physical temperature, T, and transformed temperature, θ, respectively. Kirchhoff transformation temperature, T_S, is taken to be 300 K.

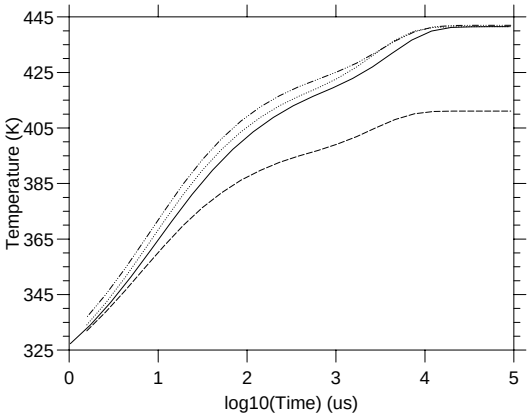

Fig. 2. Temperature rise with time ($\log_{10}(t)$ μs), for a $0.1L \times 0.1L$ square heating element, at the top surface of a cubic die, side $L = 400$ μm. Step-input power dissipation is 0.4 W. The results are calculated using an exact thermal impedance matrix solution of the time-dependent heat diffusion equation. (i) solid line, $T(t)$ (ii) dotted line, $T(\tau)$ (iii) dashed line, $\theta(\tau)$ (iv) dot-dashed line, linearisation about a typical operating point.

die, side $L = 400$ μm. Such a configuration is illustrative of, for example, a multi-finger power FET.

Eq. (4), for the integral transformation implies

$$\frac{dt}{d\tau} = \frac{k_S}{k\left(\theta(\tau)\right)} \quad \text{with} \quad t = 0 \quad \text{for} \quad \tau = 0, \tag{6}$$

so as $k\left(\theta(\tau)\right)$ is known from the analytical thermal impedance matrix solution, Eq. (6) implies that physical time, t, can be obtained in terms of transformed time, τ, by simple 1-dimensional numerical integration. Hence $\theta(t)$ is immediately recovered. Then performing the inverse of the Kirchhoff transformation, which is easily achieved analytically [5], physical active device temperatures are finally obtained as a function of physical time, $T(t)$. Fig. 2, shows curves for the full, physical solution, $T(t)$, after both inverse Kirchhoff and time variable transformations (solid line); the partially transformed solution, $T(\tau)$, after inverse Kirchhoff transformation, but assuming constant diffusivity, $k(\theta) = k_S$ (dotted line); and transformed solution $\theta(\tau)$ neglecting both the inverse Kirchhoff and time variable transformations, *i.e.*, assuming the thermal problem for the GaAs die is effectively fully linear (dashed line).

It is apparent that total neglect of thermal non linearity leads to a ∼30 K underestimate (dashed line) of the steady-state temperature rise of ∼140 K (solid line). Including the inverse Kirchhoff transformation, but neglecting the inverse time variable transformation (dotted line) is seen to overestimate the temperature rise by ∼4 % at any given instant, or equivalently, to underestimate the rise time required to reach a given temperature by as much as ∼35 %.

Fig. 2 also shows a fourth curve (dot-dashed line), illustrating the sometimes used approximation of effectively linearising the time-dependent heat diffusion equation about a typical operating point, without employing either the Kirchhoff or the time variable transformation. This curve is obtained by assuming a constant diffusivity, k_S, but with constant conductivity, κ_S, adjusted to reflect the reduced value at elevated temperatures. Choosing $\kappa_S = 36.0$ W/m.K corresponding to a temperature of 366.8 K, instead of $\kappa_S = 46.0$ W/m.K corresponding to a temperature of 300 K, gives a calculated steady-state response accurate to within 0.5 K. However, it is apparent that the error in this approximation is greater than that obtained by invoking the Kirchhoff transformation, but neglecting the time variable transformation (dotted line). Also, whereas $T(t)$ (solid line), $T(\tau)$ (dotted line) and $\theta(\tau)$ (dashed line), all tend to the same values at small times and temperature rises, the fourth curve (dot-dashed line) shows a systematic overestimate of temperature for all times compared to the full numerical result (solid line). The error in the fourth approach corresponds to ∼6 % overestimate of temperature rise, or underestimate of rise time by as much as ∼60 %. In addition, simply guessing a suitable operating point for linearisation is highly subjective, and for the case of transient thermal variation of large amplitude, easily leads to errors of ±5 K in the calculated steady-state operating temperatures.

Full linearisation of the time-dependent heat diffusion equation should therefore be implemented to obtain sufficient accuracy.

III. Analytical solutions

Having described the exact (not small signal) transformation of the non linear time-dependent heat diffusion equation, to produce a fully linear problem, analytical solution of the linear problem in terms of thermal impedance matrices is now described.

A. The homogeneous MMIC

An analytical solution to the linearised heat diffusion equation, Eq. (5), is constructed for the case of a homogeneous MMIC, $0 < x < L$, $0 < y < W$, $0 < z < D$, with active device elements $i = 1, ..., M$ described by surface elementary areas, D_i. Adiabatic boundary conditions are assumed on the side faces and a generalised 'radiation' boundary condition is imposed on the top and bottom faces, $z = 0, D$. This can be written,

$$\alpha_{0,D}\kappa_S \frac{\partial\theta}{\partial z} + H_{0,D}\left(\theta - \theta_{0,D}(x,y,t)\right) + p_{0,D}(x,y,t) = 0. \tag{7}$$

Non linear boundary conditions can be treated in the limit of a sequence of such fully linear problems [4], [23]. Here, imposed flux densities $p_{0,D}(x,y,t)$ are time dependent. Coefficients $H_{0,D}$ describe surfaces fluxes due to radiation and convection. The $\alpha_{0,D}$ equal zero for imposed temperature boundary conditions and unity for imposed flux boundary conditions. The respective ambient temperatures ($\alpha_{0,D} \neq 0$), or heatsink mount temperatures ($\alpha_{0,D} = 0$), are also dependent on time, $\theta_{0,D}(x,y,t)$. The generality of this boundary condition allows vertical matching of thermal subsystems, by interface discretisation and thermal impedance matrix manipulation, as well as integral treatment of surface fluxes.

To solve this problem, the Laplace transform is constructed giving,

$$\nabla^2\overline{\theta} - \frac{1}{k_S}\left[s\overline{\theta} - \theta(t=0)\right] = 0, \tag{8}$$

assuming no volume sources or sinks, and describing surface fluxes by imposed boundary conditions, Eq. (7).

For the case of a uniform initial temperature distribution equal to uniform and time independent ambient temperature, the substitution

$$\overline{\Theta} = s\overline{\theta} - \theta(t=0) \tag{9}$$

is made, giving

$$\nabla^2\overline{\Theta} - \frac{s}{k_S}\overline{\Theta} = 0. \tag{10}$$

By separation of variables, the general solution for $\overline{\Theta}$ is of the form,

$$\begin{aligned}\overline{\Theta}(s) &= \sum_{mn} \cos\lambda_m x \cos\mu_n y \\ &\quad \times (C_{mn}\cosh\gamma_{mn}z + S_{mn}\sinh\gamma_{mn}z)\end{aligned} \tag{11}$$

where $m, n = 0, 1, 2, ...$, and

$$\lambda_m = \frac{m\pi}{L}, \quad \mu_n = \frac{n\pi}{W}, \quad \gamma_{mn}^2 = \lambda_m^2 + \mu_n^2 + \frac{s}{k_S}. \tag{12}$$

Such fully analytical double Fourier series solutions in Laplace transform s-space have been described previously [24]. They are to be distinguished from semi-analytical Fourier solutions in frequency space, which are based on collocation or function sampling, and require numerical manipulation such as DFT-FFT to obtain expansion coefficients [3].

With the transformation of variable, Eq. (9), the adiabatic side wall boundary conditions retain the same form and the radiation boundary condition on the top and bottom surfaces, $z = 0, D$, becomes

$$\alpha_{0,D}\kappa_S\frac{\partial\overline{\Theta}}{\partial z} + H_{0,D}\overline{\Theta} + s\overline{p}_{0,D}(x,y;s) = 0. \tag{13}$$

Within this framework, the time-dependent problem resembles very closely the time-independent problem [4], [5], thus explicit forms for the expansion coefficients are obtained from,

$$\begin{aligned}H_0 C_{mn} &= -\gamma_{mn}S_{mn}\alpha_0\kappa_S \; - \\ &\quad \frac{\int_0^L\int_0^W \cos(\lambda_m x)\cos(\mu_n y)s\overline{p}_0(x,y;s)dxdy}{\frac{LW}{4}(1+\delta_{m0})(1+\delta_{n0})}\end{aligned} \tag{14}$$

and

$$\begin{aligned}&C_{mn}\left[\alpha_D\kappa_S\gamma_{mn}\sinh(\gamma_{mn}D) + H_D\cosh(\gamma_{mn}D)\right] \\ &+ S_{mn}\left[\alpha_D\kappa_S\gamma_{mn}\cosh(\gamma_{mn}D) + H_D\sinh(\gamma_{mn}D)\right] \\ &= -\frac{\int_0^L\int_0^W \cos(\lambda_m x)\cos(\mu_n y)s\overline{p}_D(x,y;s)dxdy}{\frac{LW}{4}(1+\delta_{m0})(1+\delta_{n0})}.\end{aligned} \tag{15}$$

Here δ_{mn} is the Kronecker delta function and the standard result,

$$\int_0^L \cos\lambda_m x \cos\lambda_{m'} x\, dx = \frac{L}{2}\delta_{mm'}\left(1 + \delta_{m0}\delta_{m'0}\right), \tag{16}$$

has been used.

As in the steady state case for the homogeneous MMIC [4], [5], to illustrate a particular time-dependent form of the thermal impedance matrix, put $\alpha_0 = 1$, $H_0 = 0$ (no radiation from the top surface, $z = 0$) and $\alpha_D = 0$, $H_D = 1$, $p_D(x,y,t) = 0$, $\theta_D(x,y,t) = \theta(t=0)$ (uniform temperature on the bottom surface, $z = D$, corresponding to heat sink mounting at ambient temperature). Assume a surface power density of the form,

$$p_0(x,y,t) = \sum_i S_i(x,y)P_i(t), \tag{17}$$

where $S_i(x,y) = 1$ in active device elementary areas D_i, and $S_i(x,y) = 0$ otherwise, then

$$\overline{p}_0 = \sum_i S_i(x,y)\overline{P}_i. \tag{18}$$

The corresponding temperature distribution is given by

$$\begin{aligned}\frac{1}{s}\overline{\Theta}(s) &= -\sum_{mn}\cos\lambda_m x\cos\mu_n y \times \\ &\frac{1}{\kappa_s LW}\frac{4}{(1+\delta_{m0})(1+\delta_{n0})}\sum_i I_{mn}^i\frac{1}{\gamma_{mn}} \times \\ &\quad (\sinh\gamma_{mn}z - \tanh\gamma_{mn}D\cosh\gamma_{mn}z)\overline{P_i},\end{aligned} \tag{19}$$

with area integrals I_{mn}^i defined by

$$I_{mn}^i = \iint_{D_i}\cos\left(\frac{m\pi x}{L}\right)\cos\left(\frac{n\pi y}{W}\right)dxdy. \tag{20}$$

Constructing the surface temperatures averaged over elementary areas D_i as,

$$\overline{\Theta}_{av_i} = \frac{\iint_{D_i}\overline{\Theta}|_{z=0}\,dxdy}{\iint_{D_i}dxdy}, \tag{21}$$

immediately gives the defining equation of the thermal impedance matrix approach,

$$\overline{\theta}_{av_i} - \frac{\theta(t=0)}{s} = \sum_j R_{TH_{ij}}(s)\overline{P_j}, \tag{22}$$

where,

$$R_{TH_{ij}}(s) = \frac{1}{\kappa_S LW}\sum_{mn}\frac{4\tanh(\gamma_{mn}D)}{\gamma_{mn}(1+\delta_{m0})(1+\delta_{n0})}\frac{I_{mn}^i I_{mn}^j}{I_{00}^i}. \tag{23}$$

Extension to treat other realisations of the radiative boundary condition, Eq. (7), is immediate. This allows construction of solutions for large area substrates, with radiation and convection, and generation of series solutions for thermal subsystems with discretised interfaces, for vertical matching of thermal subvolume solutions in complex 3-dimensional systems. The expression for $R_{TH_{ij}}(s)$, Eq. (23), can be written in alternative equivalent forms [24], and is readily extended to treat N-level multilayers [24]. The temperature distribution of Eq. (19), and the corresponding thermal impedance matrix of Eq. (23), reduce to the respective steady-state forms [4], [5], in the limit $s/k \to 0$, giving for the thermal resistance matrix,

$$R_{TH_{ij}} = \frac{1}{\kappa_S LW}\left[DI_{00}^{j} + {\sum_{mn}}' \frac{4\tanh(\Gamma_{mn}D)}{\Gamma_{mn}(1+\delta_{m0})(1+\delta_{n0})}\frac{I_{mn}^{i}I_{mn}^{j}}{I_{00}^{i}}\right] \quad (24)$$

where now, $\Gamma_{mn}^2 = \lambda_m^2 + \mu_n^2$, and the sum ${\sum_{mn}}'$ is over all $m, n = 0, 1, 2, ...$ excluding $(m, n) = (0, 0)$.

The solution of the heat diffusion equation just described, provides analytical expressions for both the thermal impedance matrix and for the corresponding temperature distribution throughout the body of the MMIC. This means that once power dissipations, $\overline{P_i}$, have been obtained self-consistently, by employing the thermal impedance matrix in the coupled electro-thermal implementation, temperature can be obtained essentially exactly, if required, at any point within the body or on the surface of the MMIC. This is of value for model validation against measured thermal images.

These analytical expressions describe exactly the finite volume of the die and the finite extent of transistor fingers, without making any approximations for infinite volume or finite end effects. The elements of the matrices can be simply summed to give the total average temperature rise described by a single thermal resistance. These matrix expressions represent an essentially exact description of 3-dimensional heat flow in the body of the die.

The series solutions can be partially summed in closed form using the Watson transformation [25], and partially accelerated using the Poisson summation formula [26], to give even more rapidly evaluated expressions. These results will be presented elsewhere.

Assuming the $\overline{P_i}$ to represent step inputs of magnitude P_i, and combining tables of standard integrals, *e.g.*, [2], with expressions for the inverse Laplace transform [27], gives the time-domain form of the thermal impedance matrix,

$$\begin{aligned} &R_{TH_{ij}}(t) \\ &= \tfrac{2}{\kappa_S LW} I_{00}^{j}\left\{\sqrt{\tfrac{kt}{\pi}} + 2\textstyle\sum_{l=1}^{\infty}(-1)^l \right. \\ &\qquad \left. \times\left[\sqrt{\tfrac{kt}{\pi}}e^{-D^2l^2/(kt)} - Dl\,\mathrm{erfc}(\tfrac{Dl}{\sqrt{kt}})\right]\right\} \\ &+\tfrac{1}{\kappa_S LW}{\textstyle\sum_{mn}}' \tfrac{4}{(1+\delta_{m0})(1+\delta_{n0})}\tfrac{I_{mn}^{i}I_{mn}^{j}}{I_{00}^{i}}\tfrac{1}{\Gamma_{mn}}\times \\ &\left\{\begin{array}{r} \mathrm{erf}\left(\Gamma_{mn}\sqrt{kt}\right) - \sum_{l=1}^{\infty}(-1)^l\times \\ \left[\begin{array}{r} \exp\left\{\begin{array}{c} 2Dl\Gamma_{mn}+ \\ \ln\left[\mathrm{erfc}\left(\frac{Dl}{\sqrt{kt}}+\Gamma_{mn}\sqrt{kt}\right)\right] \end{array}\right\} \\ -\exp\left\{\begin{array}{c} -2Dl\Gamma_{mn}+ \\ \ln\left[\mathrm{erfc}\left(\frac{Dl}{\sqrt{kt}}-\Gamma_{mn}\sqrt{kt}\right)\right] \end{array}\right\} \end{array}\right] \end{array}\right\} \end{aligned} \quad (25)$$

This form of the time domain thermal impedance matrix is found to be rapidly convergent in the summation over l for all t. It is an alternative to the explicit time constant form given in [18].

Even though analytical inversion is readily achieved, numerical inversion is algorithmically simple to implement and requires only evaluation of the Laplace transform and a corresponding weight function, at a small number of real or complex s-points [28]–[31],

$$\mathcal{L}^{-1}\{f(s)\}_{t=\tau_p} = \sum_{\mu} w_\mu f(s_\mu), \quad (26)$$

with w_μ and s_μ determined uniquely for a given τ_p. Typically 5 or 6 s-points are adequate so this approach can be computationally much cheaper than analytical inversion.

Fig. 3 shows temperature rise with time at turn-on, calculated using the thermal impedance matrix approach, for cubic GaAs die of side $L = 300, 400$ and 500μm, dissipating respectively 0.3, 0.4 and 0.5 W over a central square element of side $0.1L$ on the die surface [32]. The observed

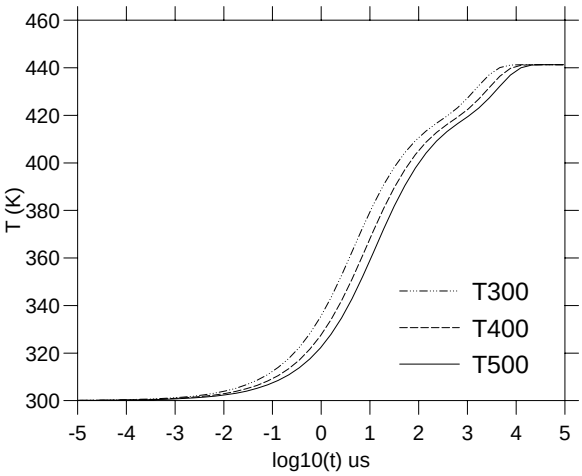

Fig. 3. Temperature rise with time at turn-on, in the immediate vicinity of the device active region in a central square, $0.1L\times0.1L$, on the surface of cubic die, side $L = 300, 400, 500$ μm, dissipating 0.3, 0.4, 0.5 W.

trend in the calculated time constant, with variation in die size, could not be predicted on the basis of commonly used thermal models, which invoke an infinite or semi-infinite substrate approximation. The significance of these results is discussed more fully in [32].

B. Volume sources

This section presents an original technique for the generation of double Fourier series solutions, describing arbitrarily distributed volume heat sources and sinks, without the use of Green's functions.

To construct the time dependent thermal solution with volume heat sources/sinks and arbitrary initial conditions, requires the solution of Poisson's equation in Laplace transform s-space. Typically, solutions with volume sources or sinks employ Green's functions techniques, but it is found advantageous in the thermal impedance matrix approach to construct such a solution by alternative means, and the solution developed for the heat diffusion problem is now outlined.

Solving the time-dependent heat diffusion equation with volume heat source in s-space,

$$\nabla^2\overline{\theta} - \frac{s}{k}\overline{\theta} = -\left[\frac{1}{\kappa}\overline{g}(x,y,z) + \frac{\theta(t=0)}{k}\right], \qquad (27)$$

and assuming a generalised double Fourier series solution of the form,

$$\overline{\theta}(s) = \sum_{mn} \cos\lambda_m x \cos\mu_n y Z_{mn}(z), \qquad (28)$$

gives,

$$\frac{d^2 Z_{mn}}{dz^2} - \gamma_{mn}^2 Z_{mn} = G_{mn}(z), \qquad (29)$$

where,

$$G_{mn}(z) = \frac{4}{(1+\delta_{m0})(1+\delta_{n0})\kappa LW} \times \int_0^L\int_0^W \cos\lambda_m x \cos\mu_n y \left[\frac{1}{\kappa}\overline{g}(x,y,z) + \frac{\theta(t=0)}{k}\right] dydx. \qquad (30)$$

To solve Eq. (29) write,

$$Z_{mn} = e^{\Gamma_{mn} z} z_{mn}, \qquad (31)$$

and make the substitution,

$$\zeta_{mn} = \frac{dz_{mn}}{dz}, \qquad (32)$$

to reduce Eq. (29) to an equation of 1^{st}-order in ζ_{mn}. This linear 1^{st}-order equation can be solved by use of a simple integrating factor, giving the general solution,

$$Z_{mn} = e^{-\Gamma_{mn} z}\int_0^z e^{2\Gamma_{mn} z'}\int_0^{z'} e^{-\Gamma_{mn} z''} G_{mn}(z'')dz''dz' + \frac{c_{1mn}}{2\Gamma_{mn}} e^{\Gamma_{mn} z} + c_{2mn} e^{-\Gamma_{mn} z}, \quad \text{for} \quad (m,n) \neq (0,0), \qquad (33)$$

(and $c_{100} + c_{200}\, z$ for $(m,n) = (0,0)$.) This solution of Eq. (29) contains two arbitrary constants so is a general solution, valid for all boundary conditions. It is to be distinguished from a Green's function solution constructed for a δ-function source, with in-built boundary conditions.

These solution techniques are individually implicit in texts such as [33]. However, the authors believe that this double Fourier series method, for treatment of arbitrary volume sources or sinks without use of Green's function techniques, represents an original approach to solution of the time-independent and time-dependent heat diffusion equations. The double series solution, Eq. (28), is to be compared with much more computationally expensive triple series solutions obtained using Green's functions. For the time-dependent case in s-space, this approach can give both small-time and large-time series solutions, which may not be readily obtainable using Green's functions. This approach is not discussed in texts such as [2], [34], [35].

This solution allows extension of the analytical thermal impedance matrix method to treat 3-dimensional volume heat sources, rather than just the planar heat sources that have been treated previously [3]–[5]. The thermal impedance matrix for power dissipating volumes, distributed arbitrarily through the body of a MMIC, is given by

$$R_{TH_{ij}}(s) = \frac{1}{\kappa LW}\sum_{mn}\frac{I^i_{mn} I^j_{mn}}{I^i_{00}}\frac{4}{(1+\delta_{m0})(1+\delta_{n0})}\frac{1}{\gamma^2_{mn}} \times \left\{ \begin{bmatrix} \frac{\sinh\gamma_{mn} z_{i2} - \sinh\gamma_{mn} z_{i1}}{\gamma_{mn}(z_{i2}-z_{i1})} \times \\ \frac{[\cosh\gamma_{mn}(D-z_{i1}) - \cosh\gamma_{mn}(D-z_{i2})]}{\cosh\gamma_{mn} D} \\ +1 - \frac{\sinh\gamma_{mn}(z_{i2}-z_{i1})}{\gamma_{mn}(z_{i2}-z_{i1})} \end{bmatrix} \right\}. \qquad (34)$$

Here, z_{i1}, z_{i2} are the z-coordinates of the planes bounding heat dissipating volume, i, in the z-direction, and the I^i_{mn} are the area integrals over the $x-y$ cross-sections, D_i, of heat dissipating volumes, i, Eq. (20). This expression is to be compared with the thermal impedance matrix for power dissipating surface areas, Eq. (23). Taking the limit, $z_{i2} \to z_{i1}$, gives the solution for a die with surface dissipating areas distributed arbitrarily throughout its volume, of value for instance in describing the buried channels below the semiconductor surface of a multi-gate power FET. Taking the further limit, $z_{i2}, z_{i1} \to 0$, reproduces the solution of Eq. (23).

This solution also makes possible treatment of the time-dependent problem for other than homogeneous initial conditions. It therefore allows construction of a time-stepping thermal impedance matrix formulation for transient electro-thermal simulations, with repeated resetting of initial conditions. Details will be presented elsewhere.

C. Rectangular N-layer

The simple descriptions of the homogeneous MMIC, presented above, are readily generalised to treat multi-layer systems by use of a transfer matrix, or two-port network, approach [36]. This is based on matching of Fourier components at interfaces, and corresponds to use of the double cosine transform to convert the 3-dimensional partial differential equation, Eq. (5), into a 1-dimensional ordinary differential equation for the z-dependent double Fourier series coefficients. Matching of linearised temperature and flux at the interfaces of a multi-layer structure can then be imposed by use of a 2×2 transfer matrix on the Fourier series coefficients and their derivatives. Arbitrary N-level structures can be treated. Different thermal conductivities can be assumed in each layer allowing treatment of composites like Cu on AlN (both having temperature independent thermal conductivities) and MMIC's with conductivities varying from layer to layer due to differences in doping levels (all layers having the same functional form for the temperature dependence of the conductivity).

The corresponding form for the thermal impedance matrix is,

$$R_{TH_{ij}}(s) = \sum_{mn}\cos\lambda_m x_j \cos\mu_n y_j \,(A_{mn}/B_{mn}) \times \frac{-4}{\kappa_1 LW(1+\delta_{m0})(1+\delta_{n0})\gamma^{(1)}_{mn}} I^i_{mn}, \qquad (35)$$

where,

$$\begin{pmatrix} A_{mn} \\ B_{mn} \end{pmatrix} = \underline{\underline{M}}^{(1)}\underline{\underline{M}}^{(2)}...\underline{\underline{M}}^{(N-1)} \begin{pmatrix} 1 \\ -\coth\gamma^{(N)}_{mn} D_N \end{pmatrix}, \qquad (36)$$

with,

$$\gamma_{mn}^{(r)} = \left(\lambda_m^2 + \mu_n^2 + \frac{s}{k_r}\right)^{1/2}, \qquad (37)$$

and the layers have thickness, D_r, thermal conductivity, κ_r, and diffusivity k_r, $r = 1, ..., N$, respectively. The $\underline{\underline{M}}^{(r)}$ are analytically obtained 2×2 matrices, determined entirely by $\kappa_r, \kappa_{r+1}, \gamma_{mn}^{(r)}, \gamma_{mn}^{(r+1)}$ and D_r.

To illustrate the accuracy and speed of this method [18], the above analytical solution for an N-level multilayer, with $s \rightarrow i\omega$, is used to plot the complex locus of the thermal transfer impedance in Fig. 4. The 4-layer, heatsink mounted device considered, is a structure examined by Szekely *et al.*, ([14] Fig. 17; [17] Figs. 5 and 6). Agreement with the calculations of Szekely seems good. The data for this figure took less than 1s to generate on a 500 MHz Pentium processor and consists of 65 frequency points.

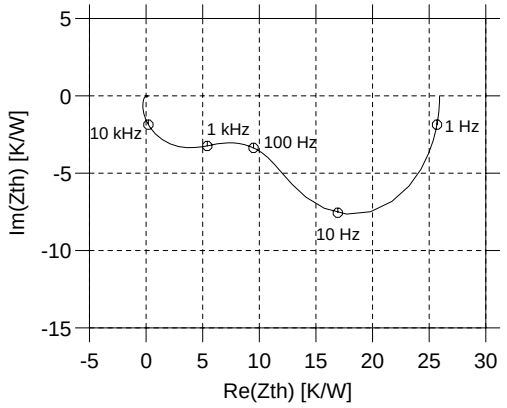

Fig. 4. Complex locus of the thermal transfer impedance, calculated using an analytical series expression, for a 4-layer, heatsink mounted structure examined by Szekely *et al.*

The method can be generalised further, by imposing specified flux discontinuities at the interfaces. The solution then represents, for instance, the case of a MMIC with active device channel buried by a thin layer of semiconductor, as described by Eq. (34) (with $z_{i2} \rightarrow z_{i1}$), but distinguishing the thermal conductivities of the various semiconductor layers.

D. MMIC superstructure

It has been demonstrated that inclusion of surface metallisation is essential for accurate description of thermal effects in power devices [37]–[39]. Comparison with experiment for multi-finger power HBTs shows that the simple thermal description corresponding to the resistance matrix of Eq. (24) is highly accurate when combined with a simple model of heat shunting by an air bridge [40]. The analytical thermal resistance and impedance matrix approach presented here, has been designed to allow descriptions of surface metallisation and air bridges, and other vertical geometries such as flip chips and solder bumps, and MMIC arrays, as outlined below.

The extension to include complex 3-dimensional structure is achieved by solving the heat diffusion equation analytically for thermal sub elements, then combining thermal impedance matrices for subsystems by matching of temperature and flux at discretised interfaces. For illustration, specifying flux on top and bottom surfaces, $z = 0, D$, and assuming no radiative or convective surface losses, ($\alpha_{0,D} = 1$, $H_{0,D} = 0$), the following relations are obtained for temperatures, $\overline{\theta}_{0\,av_i}$ and $\overline{\theta}_{D\,av_j}$, averaged over elementary areas, D_i, and D_j, on faces $z = 0$ and $z = D$, respectively,

$$\begin{aligned} \overline{\theta}_{0\,av_i} - \frac{\theta(t=0)}{s} &= \sum_{i'} R_{TH_{ii'}}^{00} \overline{P}_{0i'} + \sum_{j} R_{TH_{ij}}^{0D} \overline{P}_{Dj}, \\ \overline{\theta}_{D\,av_j} - \frac{\theta(t=0)}{s} &= \sum_{i} R_{TH_{ji}}^{D0} \overline{P}_{0i} + \sum_{j'} R_{TH_{jj'}}^{DD} \overline{P}_{Dj'}. \end{aligned} \qquad (38)$$

Here, $\overline{P}_{0i}$ and $\overline{P}_{Dj}$ are respective imposed fluxes in elementary areas, D_i and D_j, on faces $z = 0$ and $z = D$. The thermal impedance matrices are obtained in the explicit form,

$$\begin{aligned} R_{TH_{ii'}}^{00} &= \frac{1}{\kappa_S LW} \sum_{mn} \frac{-4\coth\gamma_{mn}D}{(1+\delta_{m0})(1+\delta_{n0})\gamma_{mn}} \frac{I_{mn}^{0i} I_{mn}^{0i'}}{I_{00}^{0i}}, \\ R_{TH_{ij}}^{0D} &= \frac{1}{\kappa_S LW} \sum_{mn} \frac{-4\,\mathrm{cosech}\gamma_{mn}D}{(1+\delta_{m0})(1+\delta_{n0})\gamma_{mn}} \frac{I_{mn}^{0i} I_{mn}^{Dj}}{I_{00}^{0i}}, \\ R_{TH_{ji}}^{D0} &= \frac{1}{\kappa_S LW} \sum_{mn} \frac{4\,\mathrm{cosech}\gamma_{mn}D}{(1+\delta_{m0})(1+\delta_{n0})\gamma_{mn}} \frac{I_{mn}^{Dj} I_{mn}^{0i}}{I_{00}^{Dj}}, \\ R_{TH_{jj'}}^{DD} &= \frac{1}{\kappa_S LW} \sum_{mn} \frac{-4\coth\gamma_{mn}D}{(1+\delta_{m0})(1+\delta_{n0})\gamma_{mn}} \frac{I_{mn}^{Dj} I_{mn}^{Dj'}}{I_{00}^{Dj}}, \end{aligned} \qquad (39)$$

where the I_{mn}^{0i} and I_{mn}^{Dj} are area integrals of the form, Eq. (20), over elementary areas D_i and D_j, on faces $z = 0$ and $z = D$, respectively.

These series expressions represent generalised multiport Z-parameters for the distributed thermal subsystems. Combining the thermal impedance matrices for individual subvolumes, a global thermal impedance matrix for complex 3-dimensional systems can be obtained. This is illustrated explicitly in [18] for the case of a metallised MMIC. More generally, thermal subsystems can be represented individually by netlist elements in circuit simulation. Expressing the thermal impedance matrices as non linear elements in the time domain, then allows non linear matching of interface temperatures at subsystem interfaces, in those cases where the functional form of the Kirchhoff transformation differs between subvolumes.

The s-space formulation means that no artificial piecewise constant time dependence is assumed for interface fluxes, in contrast to the time-domain USE method [2]. However, the thermal impedance matrix approach can be developed with the USE framework [7] where it avoids repeated matrix inversion.

E. Thermal vias

The analytical solution for the thermal resistance matrix has been generalised to treat, essentially exactly, full and partial thickness vias, and partial substrate thinning in power transistors and MMICs. A computationally much cheaper, but approximate, treatment of vias, based on the the simple equivalence principle method of Bonani *et al.*, [41]–[43], has also been implemented within the thermal resistance matrix approach. Construction of these solutions is described in [5].

IV. Coupled electro-thermal approach

The thermal impedance matrix in s-space can be used directly in coupled electro-thermal harmonic balance simulations. In this case the matrix of frequency dependent complex phasors corresponds to the network parameters of the distributed multi-port thermal network. It is inserted directly into the MNAM for the microwave system and so does not increase the number of non linear equations describing the coupled solution.

In the coupled electro-thermal transient problem, Laplace transformed active power dissipations, $\overline{P}_j(s)$, are not known explicitly and must be obtained by self-consistent solution. To combine the electrical and thermal descriptions, the corresponding $P_j(t)$ must therefore be discretised in time. Dividing the time interval of interest into equal subintervals of length δt, with the $P_j(t)$ taking the piecewise constant form (for illustration)

$$P_j(t) = P_j^{(n)} \quad \text{for} \quad (n-1)\delta t < t \leq n\delta t, n = 1, ..., N \quad (40)$$

then gives

$$\overline{P}_j(s) = \sum_n \frac{1}{s}(1 - e^{-s\delta t})e^{-(n-1)s\delta t}P_j^{(n)}. \quad (41)$$

Inverting the impedance matrix equation, Eq (22), the temperature rise of active element i at time $t = m\delta t$, $\Delta\theta_i^{(m)}$, is obtained as a function of the $P_j^{(n)}$. Writing $\Delta\theta_i^{(m)} = \Delta\theta_i^{(m)}(P_i^{(m)})$ from the electrical model then gives

$$\begin{aligned}
&\Delta\theta_i^{(m)}(P_i^{(m)}) \\
&= \textstyle\sum_j \mathcal{L}^{-1}\left\{R_{TH_{ij}}(s)\overline{P}_j(s)\right\}_{t=m\delta t} \\
&= \textstyle\sum_j \sum_n u(m-n+1) \\
&\times \mathcal{L}^{-1}\left\{R_{TH_{ij}}(s)\tfrac{1}{s}(1-e^{-s\delta t})\right\}_{t=(m-n+1)\delta t} P_j^{(n)} \\
&= \textstyle\sum_j \sum_n u(m-n+1) \\
&\left[R_{TH_{ij}}((m-n+1)\delta t) - R_{TH_{ij}}((m-n+2)\delta t)\right] P_j^{(n)}
\end{aligned} \quad (42)$$

where u is the unit step function,

$$u(x) = \begin{cases} 0, & x < 0 \\ 1, & x \geq 0 \end{cases}, \quad (43)$$

and the $P_j^{(n)}$ are fluxes at timesteps, n. This corresponds to N systems of equations in M unknowns, where N is the number of discretised time points in the time interval under consideration, and M is the number of heating elements. The Laplace inversion, with piecewise constant power dissipation, avoids any explicit convolution operation.

The entire thermal description is therefore obtained by precomputation of $R_{TH_{ij}}(t)$ at timesteps, $t = m\delta t$, $m = 0, ..., N$. These precomputed values can be stored for repeated re-use in different electro-thermal simulations. For reduction of precomputation time, the $R_{TH_{ij}}(t)$ can be generated at intervals, and interior points obtained accurately by interpolation. This is a time-domain approach equivalent to representation of a frequency space transfer function by a polynomial fit.

Extension to linear, quadratic or higher order interpolation of the active device power dissipations in each subinterval, δt, is immediate, and for sufficiently short step lengths, low orders of interpolation should be required.

After self-consistent electro-thermal solution, and inversion of the Kirchhoff and time variable transformations, physical active device temperatures are finally obtained as a function of physical time, $T_i(t)$, and electrical solutions, DC or RF, are determined.

V. Device Simulation

To illustrate the value of the analytical thermal impedance matrix approach for coupled electro-thermal simulations, the fully physical simulation of power FET's is now described for the time-independent case. The thermal resistance matrix model is coupled to the Leeds Physical Model (LPM). This is a quasi-2-dimensional model of MESFET's and HEMT's [8]–[11]. It makes fully physical prediction of device performance based solely on specified layer compositions and doping levels and details of the device cross-section. It is thermally self-consistent, with device self-heating described by a temperature dependent mobility. The LPM requires no prior experimental device characterisation.

For the coupled electro-thermal solution, transistor action described by the thermally self-consistent device model gives the non linear relation,

$$\Delta\theta_i = \Delta\theta_i(P_i). \quad (44)$$

Here, the Kirchhoff transformation has been applied to obtain the function $\Delta\theta_i(P_i)$ from the physical temperature dependence of the model, so thermal non linearity has been shifted from the thermal model to the already non linear active device model. Combining the active device model, Eq. (44), with the global thermal description gives

$$\Delta\theta_i(P_i) = \sum_j R_{TH_{ij}}P_j \quad (45)$$

which is a small, simple, non linear system to be solved self-consistently for the power densities, P_j. Having obtained the P_j at each bias point, from solution of the coupled electro-thermal problems, Eq. (45), by a simple relaxation algorithm, the full electrical solution is obtained and I-V curves are plotted. The temperature over the surface of the die, at a specified bias point, is obtained analytically once individual finger power dissipations have been obtained self-consistently.

Simulations are described of a 10-finger power HEMT provided by Filtronic plc. [6]. In particular, these calculations are used to ascertain the minimum physical description compatible with accurate construction of the thermal resistance matrix, e.g. inclusion of surface metallisation, air bridges, vias or surface flux losses. To allow assessment of the thermal impact on device performance of changes in parameters, the thermal resistance must be constructed from a physical model. This section describes application of the physical construction of the thermal resistance matrix for 10-finger Filtronic power HEMT FP4000, and its use in systematic study of the effects of substrate thinning, surface metallisation, vias and surface flux losses, on active channel temperatures.

Flux losses from the surface of a die can, in principle, act to reduce the thermal resistance. Radiative losses are easy to estimate and are orders of magnitude too small to have any significant impact [4]. If convective losses are of the same order of magnitude as radiative losses, then these too are insignificant. However, the magnitude of convective losses from small areas with fine surface structure are

not easily estimated. Standard correlations from the literature tend to be for large area substrates. In the absence of a detailed model of fluid flow, significant convective losses from the die surface could not be totally discounted, however these effects have not been suggested in the literature as significant at the scale of the FP4000 die.

The effect of substrate thinning on device performance was examined, and two sets of simulations were performed for dies of differing substrate thicknesses, one set including convective losses, one set excluding convective losses. The results of these simulations are described below. Figure 5 shows I-V curves calculated on the assumption of a 6 μm thick *uniform* layer of metallisation covering the whole of the power FET surface. This is a reasonable approximation in the case of the heavily metallised FP4000. Zero surface convection and a 75 μm thick substrate were assumed. A full suite of I-V curves took around 30 minutes to produce on a 500 MHz Pentium processor.

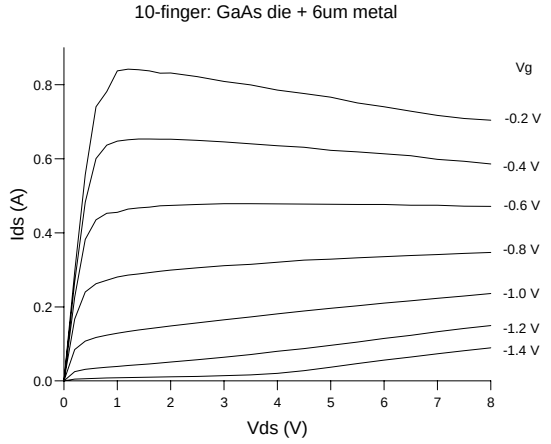

Fig. 5. Electro-thermally simulated I-V characteristics of the 10-finger Filtronic power HEMT with *6 μm surface metallisation and adiabatic surface boundary conditions*. Finger width is 400 μm; substrate thickness is 75 μm; heatsink temperature is 300 K.

Power dissipation at a bias point $(V_{DS}, V_G) = (3.5V, -0.2V)$ was calculated to be 2.8 W, and temperature at the metal-GaAs interface was calculated to vary from 27°C to 67°C. The simulation was repeated for a 400 μm thick substrate. At the same bias point, power dissipation was then found to be 2.1 W and interface temperature varied from 71°C to 127°C.

Figure 6 shows simulated temperature at the GaAs/metal interface, i.e. in the layer of the active device channels, for FP4000 with substrate thickness of 75 μm, but now assuming strong surface convection. Power dissipation is 3.0 W and temperature varies from 27 °C to 49 °C.

A further simulation of temperature at the GaAs/metal interface for FP4000 with substrate thickness of 400 μm and strong surface convection gave very similar results. Power dissipation at the same bias point was calculated to be 2.9 W and temperature varied from 27 °C to 54 °C.

The effect of including a strong convective surface flux is to make active device temperature largely independent of substrate thickness, in contrast to the zero flux case.

Simulations constructed thermal resistance matrices for a bare GaAs die, a die with surface metallisation, a metallised die with vias, and a metallised die with strong surface convection. Vias were calculated to have negligible impact on thermal calculations of device performance. Sur-

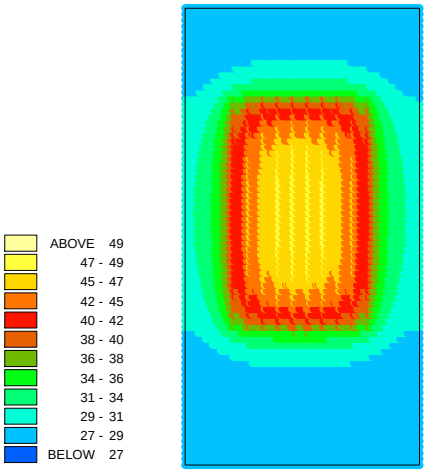

Fig. 6. Electro-thermally simulated interface temperature plot of the 10-finger Filtronic power HEMT with *6 μm surface metallisation and convective surface fluxes*. Finger width is 400 μm; *substrate thickness is 75 μm*; heatsink temperature is 300 K. Bias point is (V_{DS}, V_G) = (3.5 V, -0.2 V); power dissipation is 3.0 W. Temperature varies from 27 °C to 49 °C.

face metallisation was shown to have a heat spreading effect, reducing die peak temperatures and the corresponding thermal droop in I-V curves. These electro-thermal results are in agreement with previous thermal calculations [37]–[39],[41]–[44]. Increased substrate thickness, in the absence of convection, was seen to imply increased surface temperature. Imposition of large surface convective fluxes appeared unphysical as they implied surface temperature profiles largely independent of substrate thickness, in contrast to results obtained experimentally.

VI. Circuit simulation

Having demonstrated fully physical device level simulation, based on the thermal resistance matrix approach for the time-independent case, circuit level simulation based on the time-dependent thermal impedance matrix is now illustrated, by combination with microwave circuit simulator, Transim (NCSU) [19].

A. Transim (NCSU)

Transim has an input format that is similar to the SPICE format with extensions for variables, sweeps, user defined models, and repetitive simulation. The program provides a variety of output data and plots. Transim allows the addition or removal of new circuit elements in a very simple way. It is designed so that new circuit elements can be coded and incorporated into the program without modification to the high-level simulator. It is also quite simple to add a new analysis type. Some insight into the program architecture is given in [19]. Simulations were performed using state variable harmonic balance [45] and convolution transient [46] methods.

Thermal effects were incorporated into the circuit simulator engine by making the thermal model look like an electrical circuit [47], specifically a multi-port network described in either the time or frequency domain. To ensure separate circuits for the electrical and thermal subsystems. a local reference node concept was employed. This was initially developed for integrated circuit and field analysis of

distributed microwave circuits [48], and guarantees that there is no mixing of electric and thermal currents.

As a result of the fully analytical description of thermal subsystems, implemented as multi-port elements within Transim, no separate thermal simulator is required to characterise the thermal system, prior to coupled electro-thermal simulation by the simulation engine.

B. 3×3 MMIC array

Simulations are described of a MMIC grid array representative of one kind of spatial power combining architecture. For illustration, this consists of a 3×3 array of GaAs dies, attached to an FR-4 substrate which is cooled entirely by radiation and convection (no heatsink mounting). Non linear matching of transformed temperatures is imposed at the GaAs/FR-4 interface. Transient calculations are performed for the case of a 0.2 W power step applied to the surface of each MMIC. Thermal impedance matrices are constructed in the time-domain for the MMICs and the grid array substrate. The resulting system of non linear equations is solved in Transim by a quasi-Newton method.

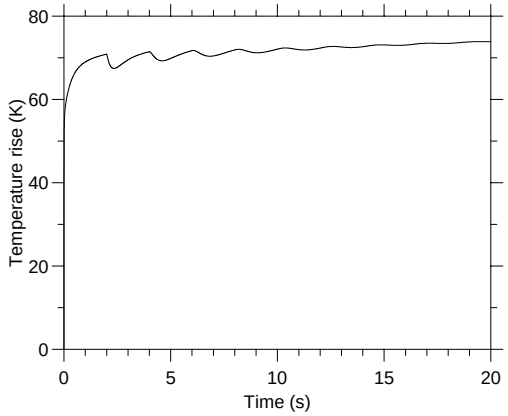

Fig. 7. Electro-thermally simulated transient response of a corner MMIC in a 3×3 GaAs on FR-4 array. A power step input of 0.2 W is applied to each MMIC.

Fig. 7 illustrates clearly two time constants. Rapid rise in temperature to 60 K above ambient is characteristic of the MMIC die. The slow ∼10 K rise over ∼20 s is due to heating of the much larger FR-4 substrate. The damped oscillations in the response are not currently fully understood. Numerical or physical reasons for this response will be described.

VII. Conclusion

An original spectral domain decomposition approach to the solution of the time-dependent heat diffusion equation, in complex 3-dimensional systems, has been described. This approach is immediately compatible with coupled electro-thermal device and circuit level simulation, on CAD timescales, by implementation in the form of analytically obtained thermal impedance matrices for thermal subsystems. These matrices have immediate interpretation in terms of multi-port thermal network parameters.

The problem of thermal non linearity, due to temperature dependent thermal diffusivity, has been treated fully for the first time in electro-thermal CAD. This required application of a time variable transformation, in addition to the well known Kirchhoff transformation for treatment of temperature dependent thermal conductivity.

A range of original thermal solutions have been presented in the form of thermal impedance matrices for electro-thermal subsystems. In particular, an original, Green's function free, approach to the double Fourier series solution of problems with arbitrarily distributed volume heat sources and sink, has been described. The construction of global thermal solutions, for complex 3-dimensional systems, based on the thermal impedance matrix approach, has been outlined.

The thermal impedance matrix approach has been illustrated by combination with the Leeds Physical Model of MESFETs and HEMTs, and by implementation in microwave circuit simulator, Transim (NCSU).

The ability to calculate trends in electro-thermal device performance with variation of physical parameters has been indicated by fully coupled, physical electro-thermal simulation of power HEMT FP4000. These results illustrate the power of modelling the temperature rise physically. The effect of vias, surface metallisation substrate thinning and surface fluxes can be predicted on the basis of device geometry and material constants.

An illustrative circuit level calculation of thermal response in a spatial power combining MMIC grid array, demonstrates clearly the range of thermal time constants implicit in simulation of large microwave systems.

The modelling capability described here will be applied to the study and design of spatial power combining architectures for use as high power sources at millimeter wavelengths.

VIII. Acknowledgements

This work was supported by the U.S. Army Research Office through Clemson University as a Multidisciplinary Research Initiative on Quasi-Optics, agreement Number DAAG55-97-K-0132.

References

[1] D. Gottlieb and S. A. Orszag, 'Numerical analysis of spectral methods: theory and applications,' CBMS-NSF Regional Conference Series in Applied Mathematics, SIAM, Philadelphia, 1977.

[2] J. V. Beck, K. Cole, A. Haji-Sheikh and B. Litkouhi, 'Heat conduction using Green's functions,' Hemisphere Publishing Corp., Washington DC, 1992.

[3] A. Csendes, V. Szekely, M. Rencz, 'An efficient thermal simulation tool for ICs, microsystem elements and MCMs: the μS-THERMANAL,' *Microelectron. J.*, vol. 29, 241–255, 1998.

[4] W. Batty, A. J. Panks, R. G. Johnson and C. M. Snowden, 'Electro-thermal modelling and measurement for spatial power combining at millimeter wavelengths,' *IEEE Trans. Microwave Theory Tech.*, vol. 47, no. 12, pp. 2574–2585, 1999.

[5] W. Batty, A. J. Panks, R. G. Johnson and C. M. Snowden, 'Electro-thermal modelling of monolithic and hybrid microwave and millimeter wave IC's,' *VLSI Design*, vol. 10, no. 4, pp. 355–389, 2000.

[6] R. G. Johnson, W. Batty, A. J. Panks and C. M. Snowden, 'Fully physical, coupled electro-thermal simulations and measurements of power FETs,' *IEEE MTT-S Internat. Microwave Symp. Dig.*, Paper TUIF-17, vol. 1, pp. 461–464, Boston, June 2000.

[7] S. David, W. Batty, A. J. Panks, R. G. Johnson and C. M. Snowden, 'Fully physical coupled electro-thermal modelling of transient and steady-state behaviour in microwave semiconductor devices,' *8th Gallium Arsenide Application Symp. (GAAS 2000)*, paper GAAS/P1 (3), Paris, October 2000.

[8] C. M. Snowden and R. R. Pantoja, 'Quasi-two-dimensional MESFET simulations for CAD,' *IEEE Trans. Electron Dev.*, vol. 36, pp. 1564–1574, 1989.

[9] C. G. Morton, J. S. Atherton, C. M. Snowden, R. D. Pollard and M. J. Howes, 'A large-signal physical HEMT model,' *IEEE MTT-S Internat. Microwave Symp. Dig.*, pp. 1759–1762, 1996.

[10] R. G. Johnson, C. M. Snowden and R. D. Pollard, 'A physics-based electro-thermal model for microwave and millimetre wave HEMTs,' *IEEE MTT-S Internat. Microwave Symp. Dig.*, vol. 3, Paper TH3E-6, pp. 1485–1488, 1997.

[11] L. Albasha, R. G. Johnson, C. M. Snowden and R. D. Pollard, 'An investigation of breakdown in power HEMTs and MESFETs utilising an advanced temperature-dependent physical model,' *Proc. IEEE 24th Internat. Symp. Compound Semiconductors*, pp. 471–474, San Diego, 1997.

[12] M. B. Steer et al, 'Global modeling of spatially distributed microwave and millimeter-wave systems,'*IEEE Trans. Microwave Theory Tech.*, vol. 47, pp. 830–839, 1999.

[13] K. C. Gupta, 'Emerging trends in millimeter-wave CAD,' *IEEE Trans. Microwave Theory Tech.*, vol. 46, pp. 747–755, 1998.

[14] V. Szekely, 'Identification of RC networks by deconvolution: chances and limits,' *IEEE Trans. Circ. Sys. I*, vol. 45, no. 3, pp. 244– 258, 1998.

[15] M.-N. Sabry, ' Static and dynamic thermal modelling of ICs,' *Microelectron. J.*, vol. 30, pp. 1085–1091, 1999.

[16] M. Furmanczyk, A. Napieralski, K. Szaniawski, W. Tylman and A. Lara, 'Reduced electro-thermal models for integrated circuits,' *Proc. 1st Internat. Conf. on Modeling and Simulation of Semiconductor Microsystems*, pp. 139–144, 1998.

[17] V. Szekely, 'THERMODEL: a tool for compact dynamic thermal model generation,' *Microelectron. J.*, vol. 29, pp. 257–267, 1998.

[18] W. Batty, C. E. Christoffersen, S. David, A. J. Panks, R. G. Johnson and C. M. Snowden, 'Steady-state and transient electro-thermal simulation of power devices and circuits based on a fully physical thermal model,' *THERMINIC 2000*, Budapest, September 2000.

[19] C. E. Christoffersen, U. A. Mughal, M. B. Steer, 'Object oriented microwave circuit simulation,' *Int. Journal of RF and Microwave CAE*, vol. 10, no. 3, pp. 164–182, 2000.

[20] W. B. Joyce, 'Thermal resistance of heat sinks with temperature-dependent conductivity,' *Solid-State Electronics*, vol. 18, pp. 321–322, 1975.

[21] P. D. Maycock, 'Thermal conductivity of silicon, germanium, III-V compounds and III-V alloys,' *Solid-State Electronics*, vol. 10, pp. 161–168, 1967.

[22] L. C. Wrobel and C. A. Brebbia, 'The dual reciprocity boundary element formulation for nonlinear diffusion problems,' *Comp. Meth. Appl. Mech. Eng.*, vol. 65, pp. 147–164, 1987 (and references therein).

[23] R. M. S. da Gama, 'A linear scheme for simulating conduction heat transfer problems with nonlinear boundary conditions,' *Appl. Math. Modelling*, vol. 21, no. 27, pp. 447–454, (1997).

[24] A. G. Kokkas, 'Thermal analysis of multiple-layer structures,' *IEEE Trans. Electron Devices*, vol. ED-21, no. 11, pp. 674–681, 1974.

[25] A. D. Wunsch, 'Complex Variables with Applications,' 2nd Edition, (Appendix to Chapter 6), Addison-Wesley, 1994.

[26] H. Dym and H. P. McKean, 'Fourier Series and Integrals,' Academic Press, New York, 1972.

[27] F. Oberhettinger and L. Badii, 'Tables of Laplace Transforms,' Springer-Verlag, 1973.

[28] H. Stehfest, 'Algorithm 368 Numerical inversion of Laplace transforms [D5],' *Comm. ACM*, vol. 13, no. 1, pp. 47–49 and 624, 1970.

[29] P. Satravaha and S. Zhu, 'An application of the LTDRM to transient diffusion problems with nonlinear material properties and nonlinear boundary conditions,' *Appl. Math. Comp.*, vol. 87, no. 2–3, pp. 127–160, 1997.

[30] K. Singhal and J. Vlach, 'Computation of time domain response by numerical inversion of the Laplace transform,' *J. Franklin Inst.*, vol. 299, no. 2, pp. 109–126, 1975.

[31] R. Griffith and M. S. Nakhla, 'Mixed frequency/time domain analysis of nonlinear circuits,' *IEEE Trans. CAD*, vol. 11, no. 8, pp. 1032–1043, 1992.

[32] W. Batty, A. J. Panks, S. David, R. G. Johnson and C. M. Snowden, 'Electro-thermal modelling and measurement of thermal time constants and natural convection in MMIC grid arrays for spatial power combining,' *IEEE MTT-S Internat. Microwave Symp. Dig.*, vol. 3, pp. 1937–1940, 2000.

[33] Rektorys Karel, 'Survey of Applicable Mathematics,' Iliffe, London, 1969.

[34] H. S. Carslaw and J. C. Jaeger, 'Conduction of Heat in Solids,' 2nd Edition, Oxford University Press, 1959.

[35] M. N. Ozisik, 'Heat Conduction,' Wiley, New York, 1980.

[36] J.-M. Dorkel, P. Tounsi and P. Leturcq, 'Three-dimensional thermal modeling based on the two-port network theory for hybrid or monolithic integrated power circuits,' *IEEE Trans. Components, Packaging and Manufacturing Technology – Part A*, vol. 19, no. 4, pp. 501–507, 1996.

[37] P. W. Webb and I. A. D. Russell, 'Thermal resistance of gallium-arsenide field-effect transistors,' *IEE Proc.*, vol. 136, pt. G, no. 5, pp. 229–234, 1989.

[38] P. W. Webb and I. A. D. Russell, 'Thermal simulation of transients in microwave devices,' *IEE Proc.*, vol. 138, pt. G, no. 3, pp. 329–334, 1991.

[39] P. W. Webb, 'Thermal modeling of power gallium arsenide microwave integrated circuits,' *IEEE Trans. Electron Dev.*, vol. 40, no. 5, pp. 867–877, 1993.

[40] C. M. Snowden, 'Large-signal microwave characterization of AlGaAs/GaAs HBT's based on a physics-based electrothermal model,' *IEEE Trans. Microwave Theory Tech.*, vol. 45, no. 1, pp. 58–71, 1997.

[41] F. Bonani, G. Ghione, M. Pirola and C. U. Naldi, 'Large-scale, computer-aided thermal design of power GaAs integrated devices and circuits,' *Proc. IEEE GaAs IC Symposium*, pp. 141–144, 1994.

[42] F. Bonani, G. Ghione, M. Pirola and C. U. Naldi, 'A large-scale, self-consistent thermal simulator for the layout optimization of power III-V field-effect and bipolar transistors,' *IEEE GaAs '94, Proc. European Gallium Arsenide and Related III-V Compounds Applications Symp.*, pp. 411–414, 1994.

[43] F. Bonani, G. Ghione, M. Pirola and C. U. Naldi, 'Thermal CAD for power III-V devices and MMICs,' *Proc. SBMO/IEEE MTT-S Internat. Microwave and Optoelectronics Conf.*, vol. 1, pp. 352–357, 1995.

[44] P. W. Webb, 'Thermal design of gallium arsenide MESFETs for microwave power amplifiers,' *IEE Proc.-Circuits Devices Syst.*, vol. 144, no. 1, pp. 45–50, 1997.

[45] C. E. Christoffersen, M. B. Steer and M. A. Summers, 'Harmonic balance analysis for systems with circuit-field interactions,' *IEEE Int. Microwave Symp. Dig.*, pp. 1131-1134, June 1998.

[46] C. E. Christoffersen, M. Ozkar, M. B. Steer, M. G. Case and M. Rodwell, 'State-variable-based transient analysis using convolution,' *IEEE Trans. Microwave Theory Tech.*, vol. 47, no. 6, pp. 882–889, 1999.

[47] H. Gutierrez, C. E. Christoffersen and M. B. Steer, 'An integrated environment for the simulation of electrical, thermal and electromagnetic interactions in high-performance integrated circuits,' *Proc. IEEE 6th Topical Meeting on Electrical Performance of Electronic Packaging*, Sept. 1999.

[48] C. E. Christoffersen and M. B. Steer 'Implementation of the local reference concept for spatially distributed circuits,' *Int. J. of RF and Microwave Computer-Aided Eng.*, vol. 9, no. 5, 1999.